

# SATELLITE SYNTHETIC APERTURE RADAR SEA SURFACE DOPPLER MEASUREMENTS

**B. Chapron<sup>1</sup>, F. Collard<sup>2</sup>, and V. Kerbaol<sup>2</sup>**

<sup>1</sup>Laboratoire d'Océanographie Spatiale, IFREMER

<sup>2</sup>BOOST-Technologies, Plouzané, France

## ABSTRACT

For the first time, global line-of-sight synthetic aperture radar (SAR) Doppler measurements over ocean scenes have been systematically extracted and carefully analyzed. This unique opportunity follows the enhanced sampling and processing capabilities offered by the ENVISAT ASAR instrument for the so-called Wave Mode products. Using precise satellite platform orbital and state vector parameters, measurable SAR Doppler frequency shifts can be globally obtained. From a theoretical analysis and co-located atmospheric wind and wave model predictions, these line-of-sight Doppler shifts are shown to carry valuable quantitative information about the expected mean motion between the sea scatters and the satellite platform. To further illustrate the use of these measurements, the analysis is carried out to larger SAR image complex products over coastal regions. Sub-tiling the larger SAR scenes to compute local estimates, the line-of-sight Doppler variations can be connected to local environmental parameter changes (wind, wave, current). Such a capability from standard SAR instruments shall help the developments of new and more consistent SAR retrieval algorithms for scientific and practical application purposes.

Key words: Ocean surface SAR measurements; line-of-sight Doppler frequency shifts; mean sea scatter motions.

## 1. INTRODUCTION

The circulation of the ocean's surface layer has traditionally received much attention. An important feature of this surface circulation is the motion associated with surface gravity waves and wind drift. In that context, remote sensing and especially Synthetic Aperture Radar (SAR) observations have already been demonstrated to routinely provide information to both detect oil spills and to extract different ocean surface parameters, such as surface wind, swell direction and amplitude. Over ocean scenes, SAR ocean surface remote sensing analysis indeed relies on the very high sensitivity of radar backscatter signal linked to changes on both the local geometry and the spectral density distribution of gravity-capillary ocean wavelets.

Modifications of the short surface waves by the surface layer winds, air/sea temperature variations over water masses, the presence of surface currents, bathymetry features, coastal plumes, and surface slick induced dampings, are common place observations within SAR ocean surface scenes. Challenges still remain to uniquely interpret such a wealth of high resolution identified patterns in terms of physical processes in the upper ocean, e.g. Romeiser et al. (2004). However, understandings and algorithms have evolved, and surface wind and long wave information as well as striking high resolution phenomena are routinely extracted from SAR ocean scenes.

But first, it must be stated that SAR processing technique principles involve the fine analysis of both phase and amplitude of the receiving scattered signals. This is crucial to discriminate returns from different surface areas within the radar illuminated scene according to their different respective Doppler frequencies. While such a key feature is implicitly known, most SAR ocean surface remote sensing studies still mostly focus on the squared magnitude backscatter signal modulation analysis, somehow neglecting the use of the complementary information carried in the phase of the received complex signals. However, time-dependent properties of moving SAR ocean scenes are measurable and exploited to unambiguously retrieve ocean surface swell propagation directions, e.g. Engen et al., 1995, Chapron et al., 2001, Johnsen et al. 2002.

These reliable results, as well as the enhanced processing capabilities offered by the ENVISAT ASAR instruments, such as global complex imagette (Wave Mode) products, triggered our interest for a more thorough analysis and uses of the direct line-of-sight SAR Doppler measurements, to revisit early concept from Shuchman (1979) and results from Van der Kooij et al. (2001). As foreseen, the goal is to extract an instantaneous apparent local line-of-sight surface velocity to be related with geophysical quantities (wind characteristics, surface current).

Clearly, one-channel radar systems are limited in comparison to multi-channel interferometric SAR, but actual satellite systems can still be used if orbital parameters are precisely known. The basic concept stems from the fact that detected moving targets produce Doppler shifts proportional to their relative velocities toward the receiving radar antenna. Over moving ocean scenes, which can

be represented as a collection of distributed targets, frequency shifts along the cross range will then be randomly distributed with space and time variations. This can limit the SAR imaging abilities, e.g. the velocity bunching phenomenon, but one can also use the expected statistical sea surface homogeneity to reliably infer the first order moment of the illuminated scene Doppler distribution, the so-called Doppler centroid. Accordingly, this shall provide the mean motion between the moving sea scatterers and the SAR platform. If properly demonstrated and interpreted, such a capability from standard satellite SAR instruments may systematically be used in conjunction with backscatter power measurements to help more consistent inversions of the sea surface local environmental characteristics. With the complementary measurements of both geometrical and dynamical properties of the sea surface, complex physical ocean surface processes will be better revealed and analyzed. As already mentioned, interests stem largely to possibly assess wind/wave and current induced surface motions, to be possibly combined with altimeter sea level estimates and/or HF radar measurements. Following, these measurements shall provide independent information to compare with numerical circulation model predictions. This can also further serve our understandings of wave dynamics in large steep seas for marine safety and offshore engineering design, as well as to better characterize air-sea interaction processes.

Our objectives are thus to ensure and demonstrate this potential. To this end, we take full advantages of the enhanced observation capabilities offered by the ENVISAT ASAR instrument to provide global highly sampled Wave Mode complex products with precise orbital parameters. Following the commission period to validate these products, systematic comparisons are made with numerical atmospheric and wave models (ECMWF, WAM). After briefly stating the theoretical background, section 2, the global Wave Mode product line-of-sight Doppler analysis is presented, section 3. The global analysis perfectly illustrates the expected high correlation between line-of-sight sea surface scatter motions and SAR Doppler centroid measurements. In section 4, illustrations and analysis are also given for larger complex image products.

## 2. THEORETICAL BACKGROUND

For SAR applications, the calculations of the wave scattering problem including the ability to predict quantitatively both the mean radar cross section and mean dynamical quantities, can be based upon an extended two-scale model. This is certainly justified when considering high resolution SAR images to exhibit wave field like patterns. In that sense, a two-scale model somehow introduces a separation between coherently imaged larger scale waves and smaller scale roughness elements controlling the mean backscatter and contrast signals. Under this two-scale description, the larger scales introduce local tilts to modify local incidence angles. This will in turn modify the wavenumber horizontal and vertical projections, the strength and the polarization of the backscatter signals. These larger scales are considered to slowly vary corresponding to the predominant surface

waves, while shorter scales may be described as sporadic or intermittent but statistically stationary in a mean sense. These latter contributions are generally rougher corresponding to steeper surface wave elements. From a statistical view point, these scales have rapidly decaying correlation functions in both time and space. The larger scale waves have instantaneous velocities and accelerations, both contributing to modulate the shorter scales, e.g. hydrodynamical modulations.

To simplify the developments, but to clearly illustrate the fundamental physics of such extended two-scale description, we consider the use of a Kirchhoff-like integral formulation, e.g. Winnebrener and Hasselman (1988), Thompson (1989) or Plant (2002). Over the slowly time varying larger tilting facet, the mean backscatter at a given location and time is then asymptotically approximated as

$$\begin{aligned} \sigma_{pq}^o(\mathbf{x}, t) &= \frac{k_o^2}{\pi \cos^2 \theta'} |g'_{pq}| e^{i\Omega_L t} \\ &\times \int_{\mathbf{x}} \langle e^{-2ik_o \cos \theta' (\xi(\mathbf{x}_1, t) - \xi(\mathbf{x}_2, t))} \\ &e^{2ik_o \sin \theta' (\mathbf{x}_1 - \mathbf{x}_2)} d(\mathbf{x}_1 - \mathbf{x}_2) \rangle \end{aligned} \quad (1)$$

where  $k_o$  incident is the impinging wavenumber,  $\xi$  the rapidly varying elevation roughness over the larger tilting facet,  $\theta'$  the local incidence angle according to the larger scale tilt-induced modulation,  $q$  and  $p$  indicate polarization and  $g_{pq}$  is a geometrical polarization function depending upon the dielectric constant and the local incidence angle. The fact that the surface at a given location  $\mathbf{x}$  and time  $t$  is not frozen is explicitly taken into account with the introduction of a phase term. The Doppler pulsation  $\Omega_L$  relates to the instantaneous dynamical characteristics, mainly horizontal and vertical velocities  $v_H$  and  $v_V$ , of the larger tilting facets, as  $\Omega_L = -2ik_o [\sin \theta' v_H(\mathbf{x}, t) + \cos \theta' v_V(\mathbf{x}, t)]$ .

In Eq. 1, the cross section is evaluated on a plane tilted according to a larger surface slope component. In this expression, the limits of the integration are somehow defining the spatial scale of the larger tilting waves. As discussed by Voronovitch (2002), under the small-slope asymptotic development, this type of solution is robust to scale separation. From numerical investigations and sufficiently short electromagnetic waves, the spatial area that is significant for the calculation of the integral is found to be limited to a small area concentrated around the origin of the surface coherence function  $\langle e^{-2ik_o \cos \theta' (\xi(\mathbf{x}_1, t) - \xi(\mathbf{x}_2, t))} \rangle$ . To further simplify this illustrative theoretical development, we consider Gaussian statistics, and the latter function simply writes

$$\langle e^{-2ik_o \cos \theta' (\xi(\mathbf{x}_1, t) - \xi(\mathbf{x}_2, t))} \rangle = e^{-4k_o^2 \cos^2 \theta' (\rho(\mathbf{0}) - \rho(\mathbf{x}))} \quad (2)$$

The time dependency is dropped when considering an overall statistical stationarity, i.e. the surface within the larger tilting scales is rougher everywhere the same at any time. Further analytical simplifications also appear when considering the surface to be differentiable. In this case, the correlation function  $\rho$  is approximated for short lags by  $\rho(\mathbf{x}) = \rho(\mathbf{0}) - m_{ss_x} \Delta x^2 / 2 - m_{ss_y} \Delta y^2 / 2$ . This is

obtained for a particular geometry with  $\Delta x$ ,  $\Delta y$  chosen to lie along and across the short scale roughness principal axis, i.e. the wind direction. Accordingly,  $mss_x$  is the slope variance along the wind direction. Such a simplification leads to an analytical solution for Eq. 1, as

$$\sigma_{pq}^o(\mathbf{x}, t) \simeq \frac{|g'_{pq}|}{2 \cos^4 \theta' \sqrt{mss_x mss_y}} e^{-\frac{\tan^2 \theta'}{2 mss_x mss_y} [mss_x \sin^2 \phi + mss_y \cos^2 \phi]} e^{i[\Omega_L + \Omega_s]t} \quad (3)$$

with  $\phi$  the angle between the wind direction and the line-of-sight plane of incidence. Note that the radar modulation transfer function is then defined as

$$m_{RAR} = \frac{1}{\sigma_{pq}^o} \frac{\partial \sigma_{pq}^o}{\partial \theta'} \quad (4)$$

and will be polarisation and incidence angle dependent, as well as wind induced roughness dependent.

In Eq. 3,  $\Omega_s$  stands for a Doppler offset associated with the dynamical properties of the more rapidly varying scales within the larger tilting and slowly varying facets. As developed under this simplified framework, this Doppler offset can be associated with an overall local mean velocity,  $\bar{c}$ , of the scales contributing the most to the surface coherence function at short spatial lags. At the asymptotic small perturbation electromagnetic solution,  $\bar{c}$  would correspond to the resonant Bragg scale phase speed. A coherently imaged facet shall thus exhibit a modified Doppler shift given by  $\Omega_s = -2k_o \bar{c} \sin \theta' \cos \phi$ . To possibly evaluate this mean velocity  $\bar{c}$ , for the Kirchhoff-like solution, the spatio-temporal change of the correlation function around its origin may be considered to yield

$$\Omega_s = -2k_o \bar{c} \sin \theta' \cos \phi \simeq -2k_o \frac{mss_{xt}}{mss_x} \sin \theta' \cos \phi \quad (5)$$

where  $mss_{xt}$  is a second order moment term related to the time and spatial derivatives of the correlation function evaluated at the origin. This term, as well as  $mss_x$  and  $mss_y$ , can be computed as a second order moment of the shorter scale surface roughness spectrum, e.g. Winnebrenner and Hasselman (1988) and Thompson (1989).

Following this development, the local reflectivity has a Doppler shift, proportional to  $\Omega_s + \Omega_L$ . This instantaneous Doppler shift adds to the nominal expected Doppler shift caused by the local geometry along with the platform velocity. The reflectivity induced extra term is a slow time varying function randomly distributed in space according to the randomness and temporal changes of the tilting larger facet velocities and slopes as probed within the radar illuminated area during the SAR integration time. The Doppler shift,  $\Omega_s$ , associated with the rapidly varying scales is modulated through local incidence angle changes  $\theta'(\mathbf{x}, t)$ . Considering the spatial averaging, second order correction related to this effect are expected to be proportional to both the second order moment  $mss_x$  of the larger waves and the RAR modulation amplitude. For the contribution of larger waves, correlation between the Doppler shift  $\Omega_L$  and, mostly tilt induced, modulated local cross section must also be considered. For instance,

wave systems travelling toward the instrument will produce higher cross sections over their forward faces associated with positive vertical velocities. From the definition of a line-of-sight velocity transfer function driven by the larger wave orbital motion, the strength of this effect on the overall mean Doppler will be proportional to both the second order moment  $mss_{xt} \simeq \bar{c} mss_x$  of the larger waves and the RAR modulation amplitude, Eq.4.

At this point, it is beyond the scope of the present note to further dwell on this development. Many known possible modulation impacts are not taken into account, e.g. hydrodynamic modulation, tilting larger wave local accelerations, short scale coherence time, ... But to summarize, a mean Doppler shift may be expected and, to first order, directly connected with an overall radar line-of-sight mean velocity,  $\bar{c}$ . Following the proposed development which encompasses quasi-specular and composite scattering mechanisms,  $\bar{c}$  roughly corresponds to the mean velocity of so-called intermediate scale surface facet slopes.

### 3. GLOBAL DOPPLER OBSERVATIONS

Using the orbit propagation software developed by ESA, a Doppler centroid can be predicted for any look angle and any orbit time. These calculations include the yaw steering law of the ENVISAT platform and careful estimate of the ASAR antenna boresight. These predicted Doppler centroid estimates are then used as references. Validations have been performed to check that the measured Doppler centroids estimated over land SAR scenes were correctly fitting the predicted Doppler centroid references. Knowing orbit parameters, we thus only need to properly estimate the fractional part of the Doppler centroid. Further, any Doppler ambiguity is removed by comparing measurement and prediction for which deviations of less than 100 hz are solely expected.

During the commission period to evaluate and validate ENVISAT ASAR Wave Mode products, over 300000 products have been analyzed. As part of the effort, ECMWF wind and wave model outputs have been systematically co-located with each ocean ASAR imagette scene. The global dataset thus corresponds to a very wide range of wind and wave conditions. As mentioned above, the expected Doppler centroid frequency is estimated using very accurate pointing angle and attitude information. Thanks to this precise orbital parameter knowledge for the ENVISAT ASAR, nominal Doppler offsets have been computed for each imagette product. These Doppler offsets have then been compared to the Doppler centroid directly computed from the measured complex signals. The analysis then refers to the difference between the expected and measured Doppler shifts.

Illustration of the global observation is given Figure 1. The global observation corresponds to September/October, 2003. As anticipated, the Doppler anomalies are shown to roughly be of opposite sign for descending and ascending tracks. The ASAR instrument is indeed a right-looking antenna, and negative (resp. positive) Doppler anomalies shall correspond to scatters go-

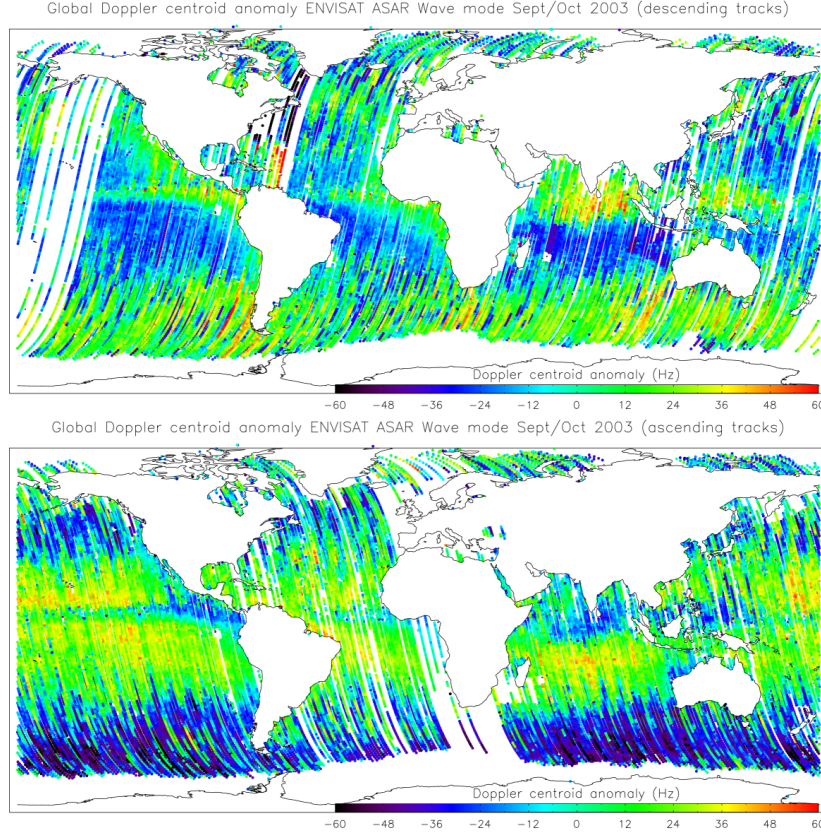


Figure 1. Frequency anomalies observation along ENVISAT ASAR descending (top) and ascending orbits

ing away from (resp. toward) the radar line-of-sight. Consequently and as revealed by this global analysis, trade winds are characterized by negative (resp. positive) frequency shifts for descending (resp. ascending) satellite passes. Clearly, the Doppler anomalies are geophysically pertinent and visually highly correlated to line-of-sight wind wave induced motions.

More quantitatively, the measured frequency shifts range from  $-50$  Hz to  $50$  Hz. Related to a mean motion by

$$\bar{c} = \frac{\pi}{k_o \sin \theta_o} \Delta f \simeq 0.064 \Delta f \quad (6)$$

a measured anomaly of about  $15$  Hz translates to a mean motion of about  $1$  m/s. Using co-located ECMWF wind estimates, a very high correlation between the frequency anomalies and the radial surface wind components is found, Figure 2. The scatter mean motion as detected by the C-band radar at  $23^\circ$  incidence angle may be linearly related to wind speed for moderate wind conditions,  $5$  m/s to  $10$  m/s. Over this range, the mean motion  $\bar{c}$  is found to lie between one fourth and one fifth of the  $10$  m surface wind speed, about  $6$  to  $8$  times the wind friction velocity. This is one order of magnitude larger than usually reported wind drift and Stokes drift estimates.

These relatively large numbers are consistent with the theoretical approximation presented in section 2. Indeed, considering a standard  $k^{-4}$  surface roughness elevation spectra and a linear dispersion relation  $c = \sqrt{g/k}$ , the mean velocity of the surface slopes may be approached

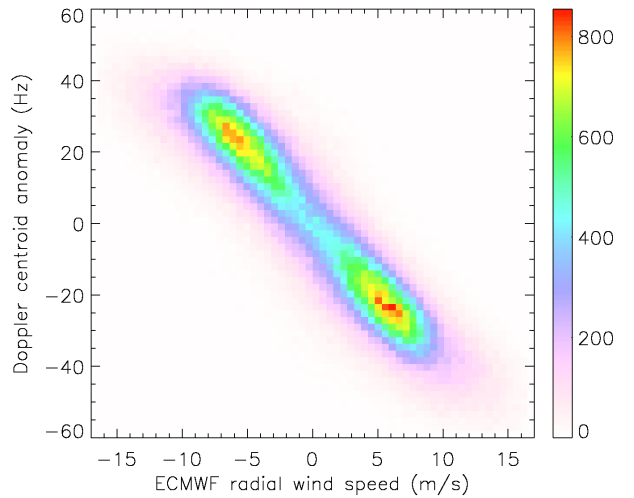


Figure 2. Correlation between the frequency anomalies and the radial surface wind components

as

$$\bar{c} \simeq \alpha c_{max} \left(1 - \frac{c_{min}}{c_{max}}\right) / \log \frac{c_{max}}{c_{min}} \quad (7)$$

For this approximation, the surface waves to be considered are those contributing the most to the surface coherence function, Eq. 2. These scales are mostly associated with the wind sea part of the elevation roughness spectrum. The larger velocity limit may be taken proportional to the wind speed, i.e.  $c_{max} \propto c_{peak} \propto U$ . The  $\alpha$  term is a proportionality constant smaller than 1 related to the definition of the spreading spectral function. For the lower velocity limit, the minimum phase speed  $c_{min}$  to be considered may be related to the friction velocity, as shorter waves may not be dispersive. From a composite electromagnetic model point, this lower limit shall correspond to facet sizes larger than 3 to 5 times the radar wavelength, i.e. 15 to 25 cm. To match Doppler anomaly measurements with a semi-empirical algorithm, the global C-band 23° ASAR observations may be approached with Eq.7, setting  $c_{max} \simeq 0.8 U$ , and  $c_{min} \simeq 0.5$  m/s.

#### 4. COASTAL OBSERVATIONS

Considering the above global analysis to successfully prove the fact that line-of-sight C-band detected sea surface scatterer motions can be readily extracted from SAR Doppler centroid measurements, it is tempting to further conduct the analysis to SAR images covering a wider area.

To this end, we report the analysis for an ENVISAT ASAR image SLC product taken over the west tip of France, Fig. 3. At the time of acquisition, the scene corresponds to relatively uniform onshore high wind conditions over an area where tidal currents are the dominant surface current contribution. Tidal currents in the area can reach  $3.5 \text{ m s}^{-1}$  for an average spring tide, with typical velocities of  $0.5 \text{ m s}^{-1}$ . Finite elements and finite differences 2-D numerical model have been applied to obtain maps of currents at 5 m depth. The tide is generated using well known harmonic constants measured in reference harbours and bottom friction is adjusted to fit observed current ellipses (Le Nestour, 1993). The tidal current at the time of the SAR scene acquisition is computed by interpolation over the one hour resolution output of the model. As observed from local estimates computed over sub-images, Fig. 3, the expected and measured Doppler frequencies are equal to zero over land. The pass is ascending, the wind is onshore, and over the sea, the mean Doppler anomaly is then found mostly negative, i.e. scatterers going away from the antenna.

More interestingly, the Doppler map exhibits local variations, e.g. between Ouessant and Molene islands in the northwestern part of the image, the Doppler anomaly almost changes sign. In this particular area, the measured mean scatterer motion is strongly reduced compared to western more open ocean conditions. Figure 4 shows the relative cross section variations over the SAR scene. As revealed, relative increases in backscatter power are generally well connected to these reduced mean scatter

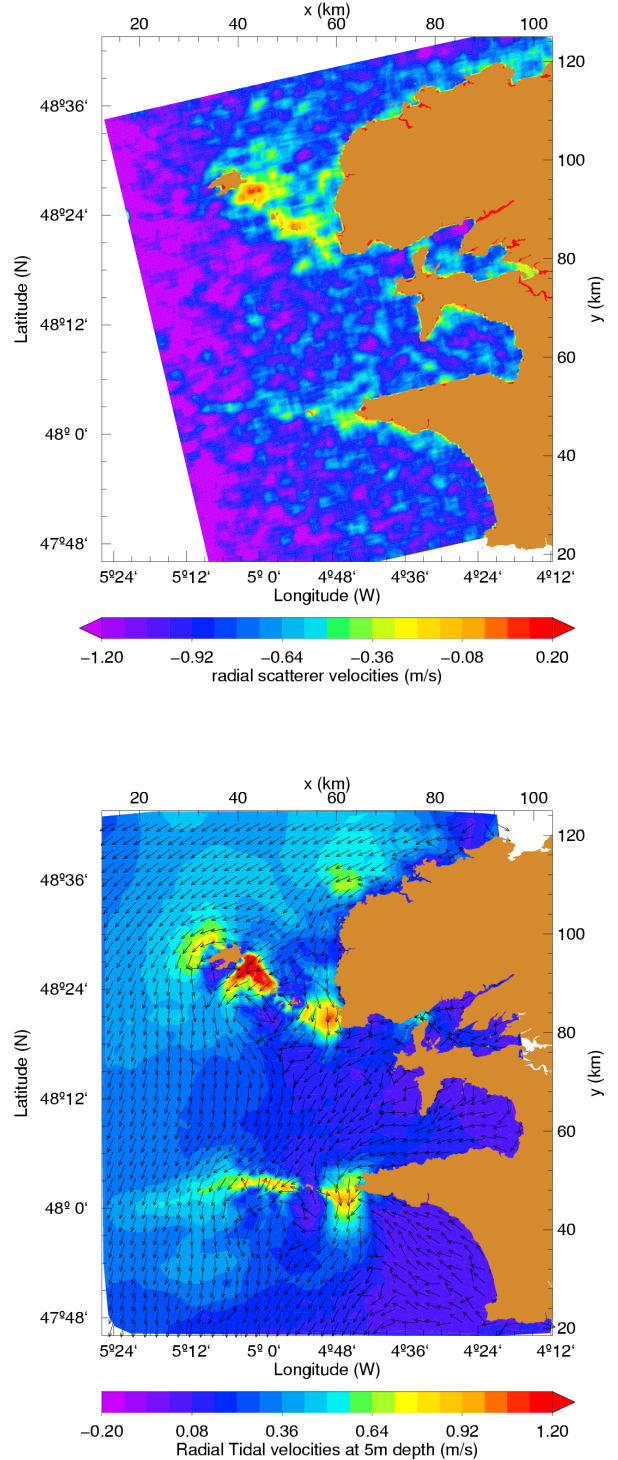


Figure 3. SAR derived horizontal scatterer velocities (top) and Model tide radial velocities

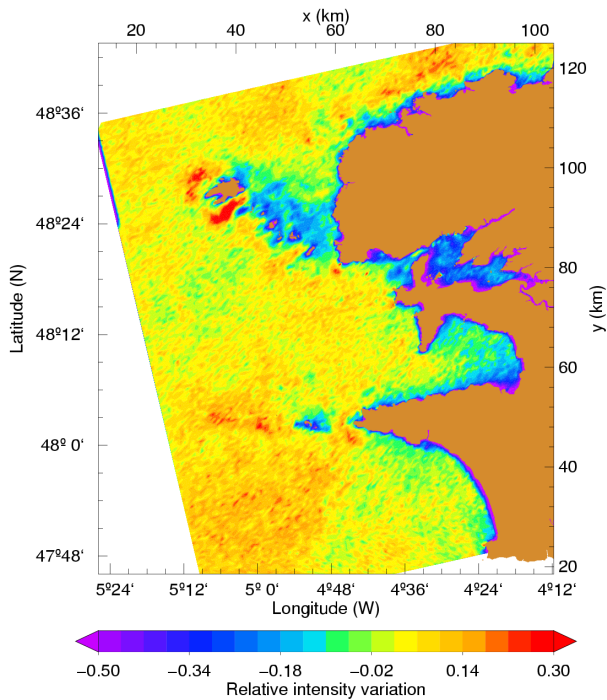


Figure 4. Relative variations of local backscatter intensity

detected motions. In this case, sea surface roughness changes are just well connected to mean surface motion changes, as certainly associated to surface current non-uniformities. The roughness transformations is usually conveniently described according to the wave action conservation, e.g. Kudryavtsev et al. (2004). In particular, adverse surface current will shorten the so-called intermediate ocean surface waves, strongly increasing the mean surface slope variance  $m_{ss_x}$ , modulating the growth rate at the surface, and thus most likely, the proportion of breaking events. The mean radar cross section will thus strongly increase. As found, estimated Doppler changes can then be ascertained to be effectively related to local environmental conditions.

## 5. OUTLOOK

Following a theoretical analysis and co-located atmospheric wind and wave model, as well as tide predictions, the line-of-sight Doppler shifts have been successfully shown to carry valuable quantitative information about the expected mean motion between the sea scatterers and the satellite platform. These global ENVISAT ASAR Wave Mode products provide a direct validation of the geophysical nature of the measured Doppler shifts. To first order, it has been theoretically derived that these shifts are dominated by an overall local mean velocity,  $\bar{c}$ , related to intermediate scale surface slope. These scales are predominantly wind driven, and in particular, these Doppler shifts have been clearly evidenced to be wind direction dependent. Magnitudes will further be polarization and incidence angle dependent according to the radar

backscatter mechanism and the related tilt and hydrodynamic radar cross section modulation transfer functions.

Changes according to surface current impacts are expected according to wave-current interaction modifications of the wind wave spectrum. As evidenced, such effects are anticipated to be very well observed under local adverse current conditions. As envisaged, combinations of both radar cross section and Doppler measurement variations shall be the key to retrieve underlying surface current characteristics.

Although the resolution may be considered low (about 1 km), the proposed synergy to infer both geometrical and dynamical properties of the sea surface shall be a sufficient independent source of remotely sensed information for most oceanographic applications. Efforts shall certainly be needed to further assess the full potential of these observations. But, such a capability from standard SAR instruments shall certainly help in the near future the development of new and more consistent retrieval algorithms for scientific and practical purposes.

## ACKNOWLEDGMENTS

We would like to acknowledge the technical support by the European Space Agency, ESA, in particular, Y.L. Desnos, B. Rosich and B. Duesman. We wish to express our gratitude to J. Closa from Altamira Inc. We further wish to acknowledge D. Hauser and A. Mouche. The coastal case study indeed benefit directly from the VALPARESO experiment to help validation/calibration of the ASAR SAR data taking place over the west tip of France (Brest). We finally thanks F. Arduin from Service Hydrographique de la Marine.

## REFERENCES

- Chapron B., H. Johnsen, and R. Garello, Wave and wind retrieval from SAR images of the ocean. *Ann. Telecommun.* 56, 11-12, 682-699, 2001
- Engen, G. and H. Johnsen, SAR-Ocean wave inversion using image cross spectra, *IEEE Trans. Geo. Rem. Sens.*, 33, 4, 1995.
- Johnsen H., Engen G., Chapron B., Walker N., Closa J., Validation of ASAR Wave Mode Level2 Product, Proc. of Envisat Cal/Val Review, *ESA SP-520*, 9-13 September 2002.
- Kudryavtsev, V. K., J. A. Johannessen, D. Akimov, O. M. Johannessen, and B. Chapron, Towards radar imaging of ocean phenomena: model and comparison with observations, *SP-565*, ESA, Noordwijk, 2004.
- R. Le Nestour, "Réalisation de l'atlas de courants de marée de la côte ouest de France, de St-Nazaire à Royan," *Tech. Report. 2*, 1993.
- W.J. Plant, "A stochastic, multiscale model of microwave backscatter from the ocean," *J. Geophys. Res.*, 2002

Romeiser R., S. Hufermann, and S. Kern, Status report on the remote sensing of current features by spaceborne synthetic aperture radar, *SP-565*, ESA, Noordwijk, 2004.

Shuchman, R., The feasibility of Measurement of Ocean Current Detection Using SAR data, Proc. of the 13th Int. Symp on Remote Sensing of the Environment, Ann Arbor, pp 93-103, 1979)

Thompson, D. R., Doppler spectra from the ocean surface with a time-dependent composite model, *Radar Scattering from Modulated Wind Waves*, ed. G.J. Komen and W.A. Oos, Kluwer Acad., Norwell Mass., 27-40, 1989

Van der Kooij M., W. Hughes, and S. Sato, Doppler current velocity measurements: A new dimension to spaceborne SAR data, available <http://www.atlantisscientific.com/eoserv.html>, 2001

A. Voronovich, "Small-slope approximation for electromagnetic wave scattering at a rough interface of two dielectric half-spaces," *Waves in Random Media*, vol. 4, pp. 337–367, 1994.

A. Voronovitch, "The effect of the modulation of Bragg scattering in small-slope approximation," *Waves in Random Media*, vol. 12, pp. 341–349, 2002.

Winnebrener, D. P. and K. Hasselmann, Specular contribution to the mean synthetic aperture radar image of the ocean surface, *J. Geophys. Res.*, 93, C8, 9281-9294, 1988